HLbL contribution to the muon $g-2$ on the lattice: overall strategy

Thomas Blum
UConn/RBRC

Norman Christ
Columbia

Masashi Hayakawa
Nagoya

Taku Izubuchi
BNL/RBRC

Luchang Jin
UConn/RBRC

Chulwoo Jung
BNL

Christoph Lehner
BNL

Cheng Tu
UConn

and the RBC/UKQCD collaborations

Mar 12, 2018
University of Connecticut
Muon g-2 Theory Initiative HLbL Working Group Workshop

Outline

- **Introduction**
- Lattice method
- HLbL on lattice
- Disconnected diagrams
- Finite volume effects
- π^0 contribution
- Summary and Future plans

Figure 1. The headstone of Julian Schwinger at Mt Auburn Cemetery in Cambridge, MA.

PHYSICAL REVIEW VOLUME 118, NUMBER 1 APRIL 1, 1960

Accurate Determination of the μ^+ Magnetic Moment*

R. L. GARWIN,† D. P. HUTCHINSON, S. PENMAN,‡ AND G. SHAPIRO§
Columbia University, New York, New York

(Received August 4, 1959)

Using a precession technique, the magnetic moment of the positive mu meson is determined to an accuracy of 0.007%. Muons are brought to rest in a bromoform target situated in a homogeneous magnetic field, oriented at right angles to the initial muon spin direction. The precession of the spin about the field direction, together with the asymmetric decay of the muon, produces a periodic time variation in the probability distribution of electrons emitted in a fixed laboratory direction. The period of this variation is compared with that of a reference oscillator by means of phase measurements of the "beat note" between the two. The magnetic field at which the precession and reference frequencies coincide is measured with reference to a proton nuclear magnetic resonance magnetometer. The ratio of the muon precession frequency to that of the proton in the same magnetic field is thus determined to be 3.1834 ± 0.0002. Using a re-evaluated lower limit to the muon mass, this is shown to yield a lower limit on the muon g factor of $2(1.00122 \pm 0.00008)$, in agreement with the predictions of quantum electrodynamics.

I. INTRODUCTION

RECENT developments in the theory of weak interactions[1] make it appear that many of the properties of the mu meson can be accounted for on the assumption that it enters into interactions in the same way as the electron but has a much larger mass. The electromagnetic properties of the muon, therefore, acquire increased interest as a further test of the identity of the interactions of the two particles.

Quantum electrodynamics[2] makes the prediction

of detecting the direction of polarization via their asymmetric decay[6] made possible the measurement of the muon magnetic moment. In the original experiment it was found necessary, to obtain agreement with the asymmetry curve, to assume a value of the moment close to the Dirac prediction. In this way the value was determined to an accuracy of 1%. The Liverpool group,[7] using an analog time-to-height converter to record the distribution in time of the emitted electrons, achieved an accuracy of 0.7%. A resonance technique, in which the muons were stopped in a large static magnetic

Current $g-2$ experiment scheme

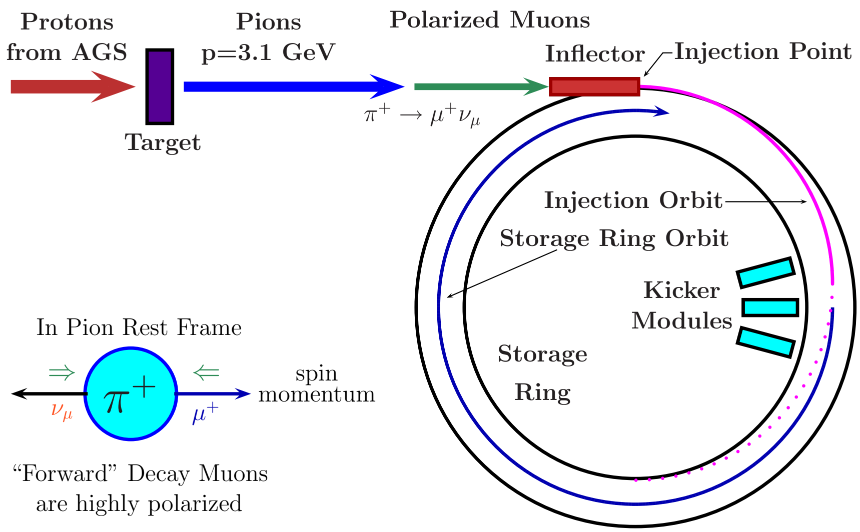

Figure 2. The schematics of muon injection and storage in the $g-2$ ring. Phys. Rept. **477**, 1 (2009).

$$\omega_c = \frac{e\,B}{m_\mu\,\gamma} \tag{1}$$

$$\omega_s = \frac{e\,B}{m_\mu\,\gamma} + a_\mu\,\frac{e\,B}{m_\mu} \tag{2}$$

$$\gamma = 1/\sqrt{1-v^2} \approx 29.3 \tag{3}$$

List of experiments

Authors	Lab	Muon Anomaly	
Garwin et al. '60	CERN	0.001 13(14)	
Charpak et al. '61	CERN	0.001 145(22)	
Charpak et al. '62	CERN	0.001 162(5)	
Farley et al. '66	CERN	0.001 165(3)	
Bailey et al. '68	CERN	0.001 166 16(31)	
Bailey et al. '79	CERN	0.001 165 923 0(84)	
Brown et al. '00	BNL	0.001 165 919 1(59)	(μ^+)
Brown et al. '01	BNL	0.001 165 920 2(14)(6)	(μ^+)
Bennett et al. '02	BNL	0.001 165 920 4(7)(5)	(μ^+)
Bennett et al. '04	BNL	0.001 165 921 4(8)(3)	(μ^-)

World Average dominated by BNL

$$a_\mu = (11659208.9 \pm 6.3) \times 10^{-10} \tag{4}$$

In comparison, for electron

$$a_e = (11596521.8073 \pm 0.0028) \times 10^{-10} \tag{5}$$

Future Fermilab E989 (0.14 ppm)

Figure 3. 1000 Piece Jigsaw Puzzle - Magnetic Moment. $18.00 from http://eddata.fnal.gov/ seems not available anymore.

Almost 4 times more accurate then the previous experiment.

J-PARC E34 also plans to measure muon $g-2$ with similar precision.

5-loops QED calculation

$$a_\mu^{\text{QED}} = 0.5 \times \left(\frac{\alpha}{\pi}\right) + 0.765\,857\,425 \underbrace{(17)}_{m_\mu/m_{e,\tau}} \times \left(\frac{\alpha}{\pi}\right)^2$$

$$+ 24.050\,509\,96 \underbrace{(32)}_{m_\mu/m_{e,\tau}} \times \left(\frac{\alpha}{\pi}\right)^3 + 130.8796 \underbrace{(63)}_{\text{num. int.}} \times \left(\frac{\alpha}{\pi}\right)^4$$

$$+ 753.29 \underbrace{(1.04)}_{\text{num. int.}} \times \left(\frac{\alpha}{\pi}\right)^5$$

$$= 116\,584\,718.853 \underbrace{(9)}_{m_\mu/m_{e,\tau}} \underbrace{(19)}_{c_4} \underbrace{(7)}_{c_5} \underbrace{(29)}_{\alpha(a_e)} [36] \times 10^{-11}$$

Aoyama et al. '12

Weak interaction contribution

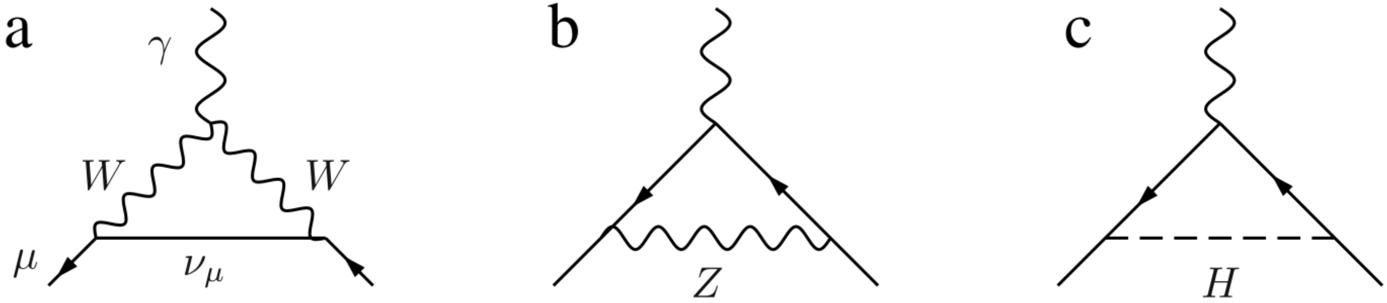

Leading weak contribution. $a = 38.87, b = -19.39, c = 0.00$ [in units 10^{-10}]

	Value ± Error	Reference
QED incl. 5-loops	11658471.8853 ± 0.0036	Aoyama, et al, 2012
Weak incl. 2-loops	15.36 ± 0.10	Gnendiger et al, 2013

Table 1. Standard model theory, QED and Weak interaction. [in units 10^{-10}]

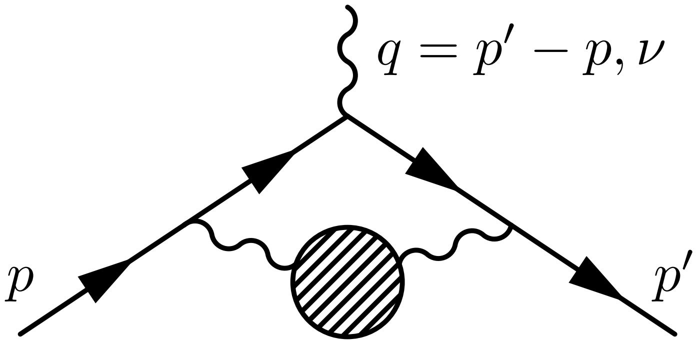

HVP: hadronic vaccum polarization

Leading order

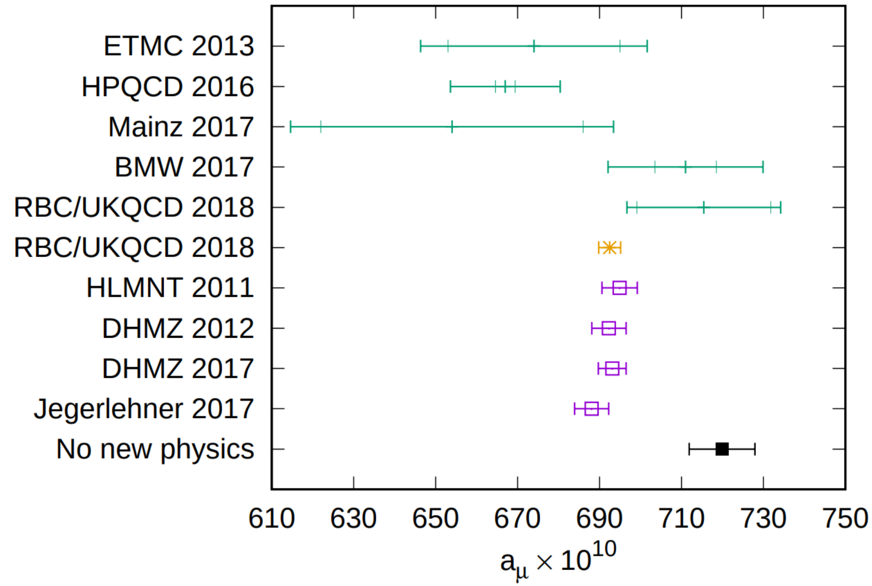

- HVP LO: Errors are being reduced quite a bit. With lattice calculation and $e^+e^- \to \text{hadrons}$ experiments data combined, We obtained 692.5 ± 2.7. **arXiv:1801.07224**.
- HVP NLO: -9.84 ± 0.07, HLMNT11. arXiv:1105.3149

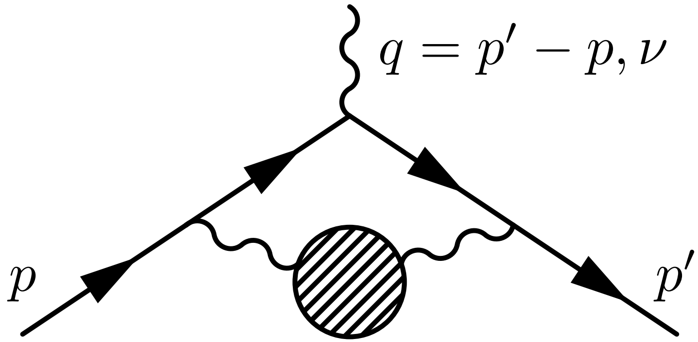

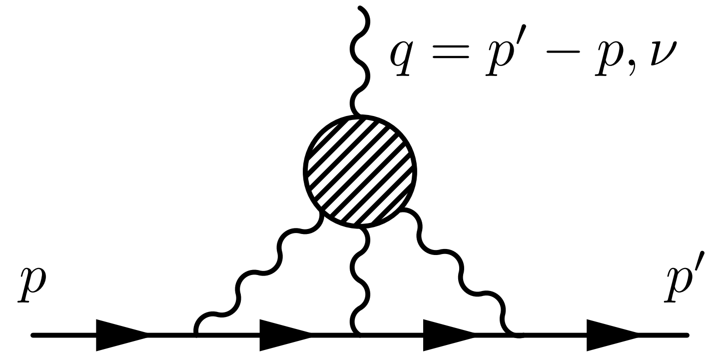

(L) HVP (R) HLbL

- HLbL: hadronic light-by-light scattering.

  The following results are obtained with combinations of models on different process.

  10.5 ± 2.6 PdRV09, Glasgow consensus, arXiv:0901.0306.

  10.5 ± 4.9 same as above, but errors added linearly instead of in quadrature.

  11.6 ± 3.9 JN09, arXiv:0902.3360.

  10.3 ± 2.9 FJ17, arXiv:1705.00263.
- Dispersive approach.
- Lattice approach.

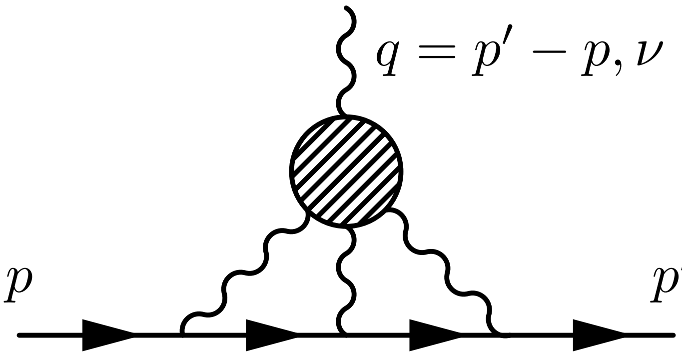

Various contributions to $a_\mu^{\mathrm{HLbL}} \times 10^{10}$

	PdRV09 (Glasgow consensus)	JN09	FJ17
π^0, η, η'	11.4 ± 1.3	9.9 ± 1.6	9.5 ± 1.2
π, K loops	-1.9 ± 1.9	-1.9 ± 1.3	-2.0 ± 0.5
axial-vector	1.5 ± 1.0	2.2 ± 0.5	0.8 ± 0.3
scalar	-0.7 ± 0.7	-0.7 ± 0.2	-0.6 ± 0.1
quark loops	0.2 (charm)	2.1 ± 0.3	2.2 ± 0.4
tensor	-	-	0.1 ± 0.0
NLO	-	-	0.3 ± 0.2
Total	10.5 ± 4.9 10.5 ± 2.6 (quadrature)	11.6 ± 3.9	10.3 ± 2.9

BNL E821 (0.54 ppm) and standard model prediction

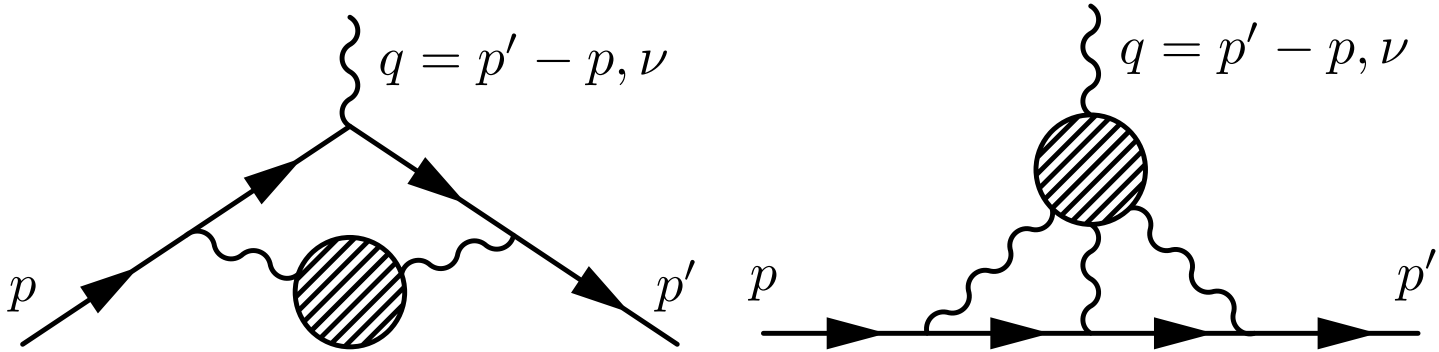

(L) HVP (R) HLbL

	$a_\mu \times 10^{10}$	
HVP ($e^+e^- \to \mathrm{hadrons}$)	692.5 ± 2.7	RBC/UKQCD and FJ17 combined
Hadronic Light by Light	10.3 ± 2.9	FJ17
Standard Model	11659180.2 ± 3.9	
Experiment (0.54 ppm)	11659208.9 ± 6.3	E821, The $g-2$ Collab. 2006
Difference ($\mathrm{Exp} - \mathrm{SM}$)	28.7 ± 7.4	

Table 2. Standard model theory and experiment comparison

There is 3.9 standard deviations!

Outline

- Introduction
- **Lattice method**
- HLbL on lattice
- Disconnected diagrams
- Finite volume effects
- π^0 contribution
- Summary and Future plans

Lattice QCD

The QCD partition function in Euclidean space time:

$$Z = \int [\mathcal{D}U_\mu] e^{-S_G[U]} \det(D[m_l, U])^2 \det(D[m_s, U]) \tag{6}$$

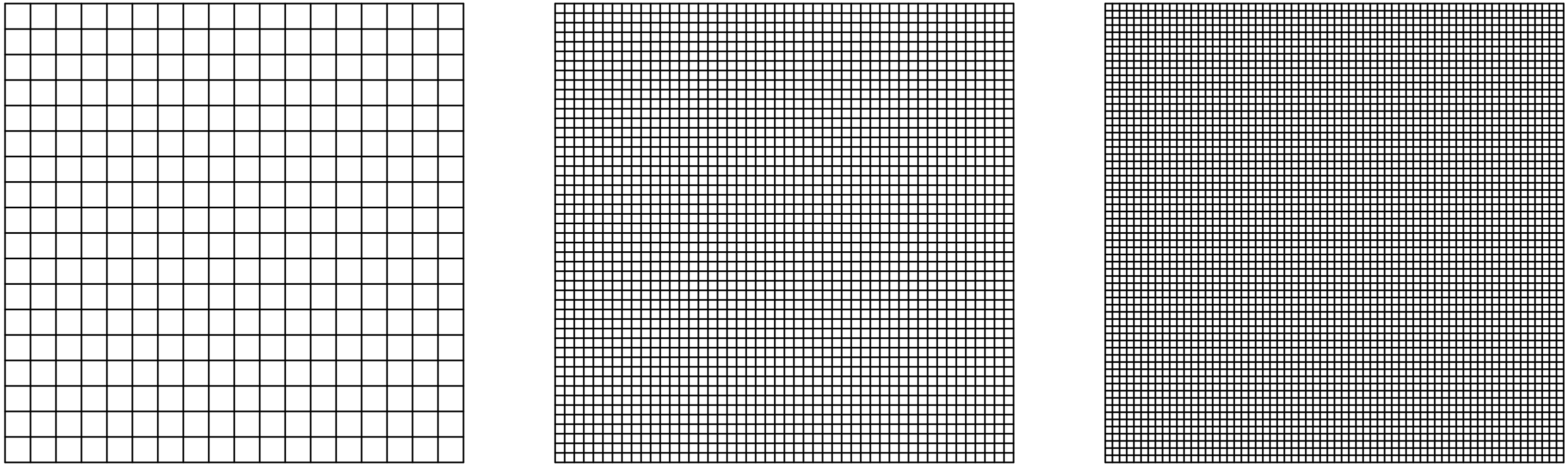

(Left) 19×19 Go board (Middle) 48×48 (Right) 64×64

The configuration is stored in position space. The reason is that the action is local in position space. Working in position makes the calculation simpler.

This is in contrast to analytical perturbative calculation, where interaction only happens occasionally. So it is advantagous to work in momentum space, where the propagator can be diagonalized.

zMobius + Multigrid Lanczos + AMA

- We are using **Domain wall fermion (DWF)** in all our lattice calculations for HLbL. DWF respects Chiral symmetry, which helps systematically eliminating the $\mathcal{O}(a)$ discretization error. The remaing discretization error are in general quite small. The fifth dimension is needed in order to fullfil the Chiral symmetry. This results numerical cost proportion to the length in the fifth dimension, L_s, and large L_s is needed to reach the Chiral limit.
- **Mobius DWF** allows us to use a smaller value for L_s and having almost the same Chiral property. For 48I, we use $L_s = 24$ to mimic the original $L_s = 48$ DWF.
- The **zMobius** formulation allows us to obtain a very good approximate of the original (M)DWF propagator with a significantly reduced L_s. For 48I, we further reduce the L_s from 24 to 10. **PoS LATTICE2015, 019 (2016)**
- **Multigrid Lanczos** algorithm help us efficiently generate the low modes of the DWF operator which accelerate the inversion roughly by a factor of 20 for light quarks. **arXiv:1710.06884**
- **All-mode-averaging (AMA)** allows us to perform the inversion with much less iterations most of the time, and only compute the small correction term for a small portion of the entire calculation. This can bring an addition factor of 5 speed up. **Phys. Rev. D 91, no. 11, 114511 (2015)**
- We use highly optimized DWF Dirac operator inverter from the **BFM** and **Grid** to perform the inversion. `https://github.com/paboyle`

Outline

- Introduction
- Lattice method
- **HLbL on lattice**
- Disconnected diagrams
- Finite volume effects
- π^0 contribution
- Summary and Future plans

- This subject is started by T. Blum, S. Chowdhury, M. Hayakawa, T. Izubuchi more than 7 years ago. **hep-lat/0509016**, **Phys.Rev.Lett. 114 (2015) no.1, 012001**.
- A series of improvements in methodology is made later. We computed the connected diagram of HLbL with 171 MeV pion mass. **Phys.Rev. D93 (2016) no.1, 014503**.
- Mainz group independently come up with a similar method to compute HLbL. **PoS LATTICE2015 (2016) 109**.
- With the improved methods, we calculated HLbL using the physical pion mass, $48^3 \times 96$, ensemble. And for the first time, we computed the leading disconnected diagrams contribution. **Phys.Rev.Lett. 118 (2017) no.2, 022005**.
- Mainz group announces the significant progress on the method to reduce the finite volume effects by treating the QED part of the HLbL diagram semi-analyticly in infinite volume. Part of the results are given in **PoS LATTICE2016 (2016) 164**.
- Encouraged by Mainz's success, we use a different approach to compute the QED part of the HLbL in infinite volume. Based the results, we exploit a way to furthur reduce the lattice discretization error and finite volume error. **Phys.Rev. D96 (2017), 034515**.

RBC's version of the history on this subject.

QED configuration v.s. Point source propagator

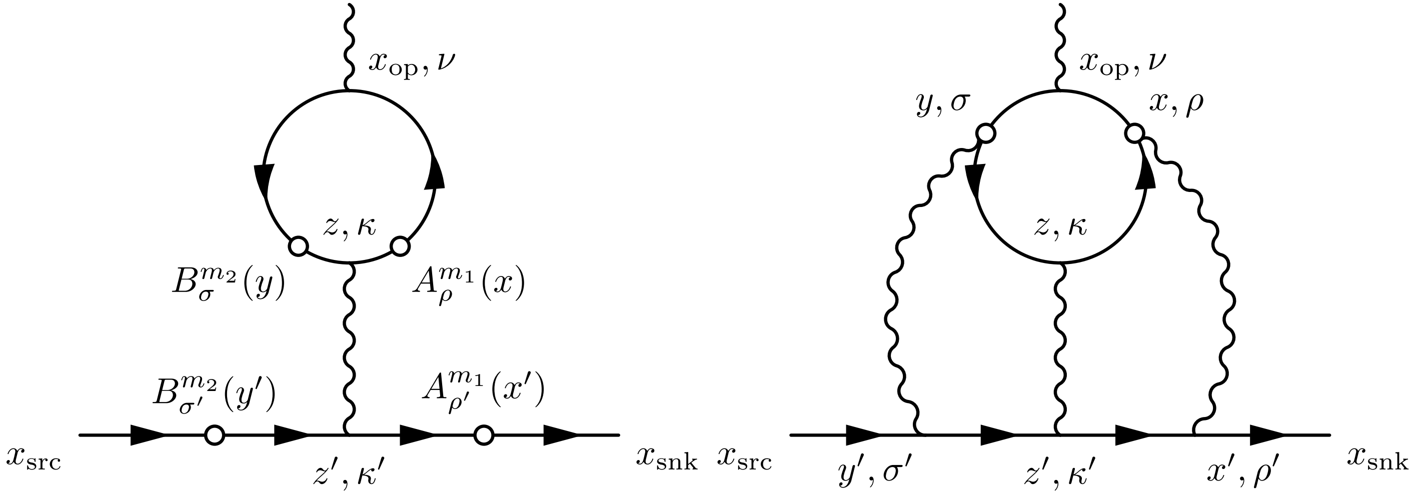

- Left: the two photon propagators are represented by ensemble average of QED configurations.
- Right: the two photon propagators are represented by random sampling of point source locations.
- Goal: Keep the signal unchanged, reduce the noise as much as possible.
- From another point of view, the question becomes: What is best way to evalute the 4 points correlation function on the lattice, which allows efficient extraction of the HLbL contribution to muon $g-2$.

Point source photon method

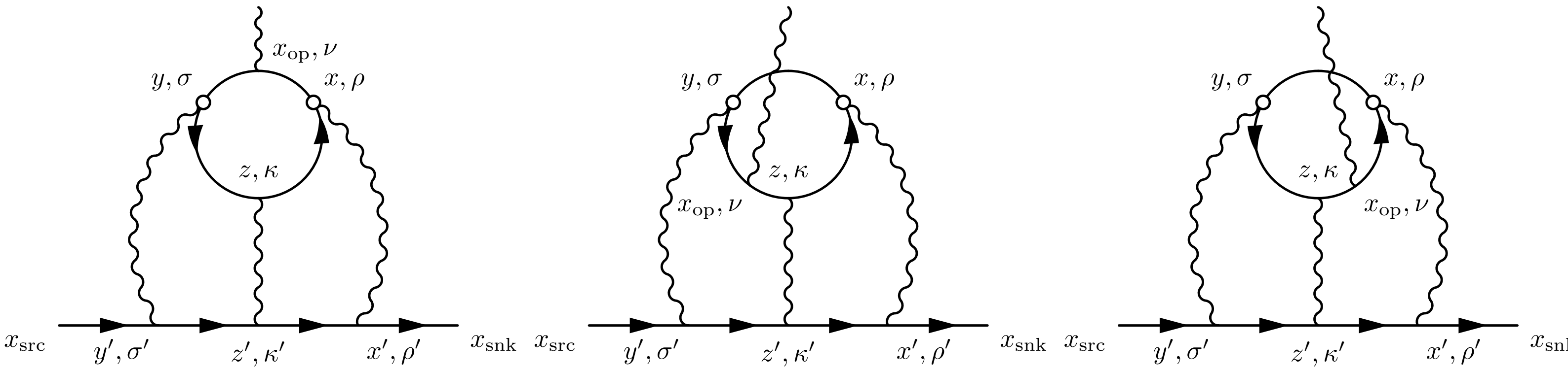

$$\mathcal{F}_\nu^C(\vec{q}; x, y, z, x_{\rm op}) = (-ie)^6 \, \mathcal{G}_{\rho,\sigma,\kappa}(\vec{q}; x, y, z) \mathcal{H}^C_{\rho,\sigma,\kappa,\nu}(x, y, z, x_{\rm op}) \tag{7}$$

$$\begin{aligned} & i^4 \, \mathcal{H}^C_{\rho,\sigma,\kappa,\nu}(x, y, z, x_{\rm op}) \\ = & \sum_{q=u,d,s} \frac{(e_q/e)^4}{6} \left\langle {\rm tr}\left[-i\gamma_\rho S_q(x, z) i\gamma_\kappa S_q(z, y) i\gamma_\sigma S_q(y, x_{\rm op}) i\gamma_\nu S_q(x_{\rm op}, x) \right] \right\rangle_{\rm QCD} \\ + & \text{ other 5 permutations} \end{aligned} \tag{8}$$

$$\begin{aligned} & i^3 \, \mathcal{G}_{\rho,\sigma,\kappa}(\vec{q}; x, y, z) \\ = & \, e^{\sqrt{m_\mu^2 + \vec{q}^2/4}(t_{\rm snk} - t_{\rm src})} \sum_{x', y', z'} G_{\rho,\rho'}(x, x') G_{\sigma,\sigma'}(y, y') G_{\kappa,\kappa'}(z, z') \\ & \times \sum_{\vec{x}_{\rm snk}, \vec{x}_{\rm src}} e^{-i\vec{q}/2 \cdot (\vec{x}_{\rm snk} + \vec{x}_{\rm src})} S_\mu(x_{\rm snk}, x') i\gamma_{\rho'} S_\mu(x', z') i\gamma_{\kappa'} S_\mu(z', y') i\gamma_{\sigma'} S_\mu(y', x_{\rm src}) \\ + & \text{ other 5 permutations} \end{aligned} \tag{9}$$

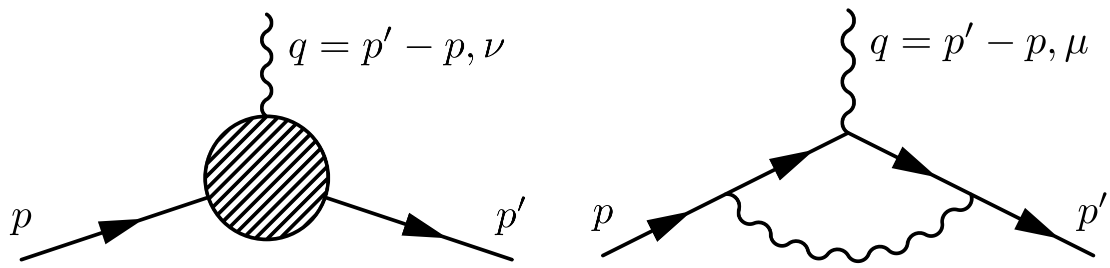

Figure 4. (L) Muon Vertex Function Diagram (R) Schwinger Term Diagram.

$$\begin{aligned}\langle \vec{p}', s' | j_\nu(\vec{x}_{\rm op} = \vec{0}) | \vec{p}, s \rangle &= \left\langle \vec{p}', s' \middle| \sum_f q_f \bar{\psi}_f(\vec{x}_{\rm op} = 0)\, \gamma_\nu\, \psi_f(\vec{x}_{\rm op} = 0) \middle| \vec{p}, s \right\rangle \\ &= -e\, \bar{u}_{s'}(\vec{p}') \left[F_1(q^2)\gamma_\nu + i \frac{F_2(q^2)}{4m} [\gamma_\nu, \gamma_\rho] q_\rho \right] u_s(\vec{p}) \end{aligned} \tag{10}$$

$$\vec{\mu} = -g \frac{e}{2m} \vec{s} = -(F_1(0) + F_2(0)) \frac{e}{m} \vec{s} \tag{11}$$

$$F_1(0) = 1 \tag{12}$$

$$F_2(0) = \frac{g-2}{2} \equiv a \tag{13}$$

Classicaly, magnetic moment is simply

$$\vec{\mu} = \int \frac{1}{2}\vec{x} \times \vec{j}\, d^3x \tag{14}$$

- This formula is not correct in Quantum Mechanics, because the magnetic moment result from the spin is not included.
- In Quantum Field Thoery, Dirac equation automatically predict fermion spin, so the naive equation is correct again!

$$\langle \vec{\mu} \rangle = \left\langle \psi \middle| \int \frac{1}{2}\, \vec{x}_{\rm op} \times i\, \vec{j}(\vec{x}_{\rm op})\, d^3x_{\rm op} \middle| \psi \right\rangle \tag{15}$$

- $i\, \vec{j}(\vec{x}_{\rm op})$ is the conventional Minkovski spatial current, because of our γ matrix convention.
- The right hand generate the total magnetic moment for the entire system, including magnetic moment from spin.
- Above formula applies to **normalizable state** with zero total current. Not practical on lattice because it need extremely large volume to evaluate.

$$L \gg \Delta x_{\rm op} \sim 1/\Delta p \tag{16}$$

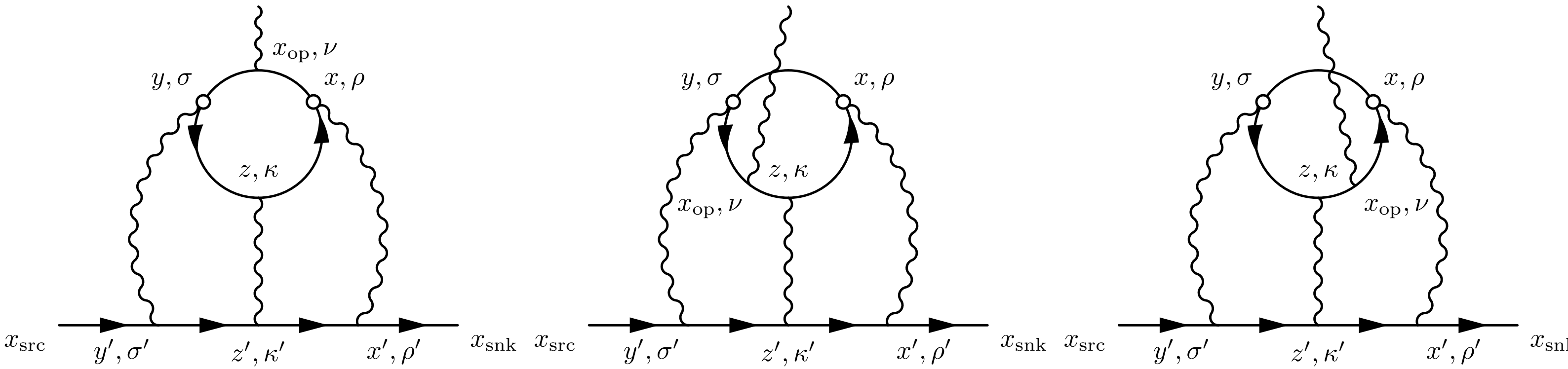

$$\frac{F_2(0)}{m}\,\bar{u}_{s'}(\vec{0})\frac{\vec{\Sigma}}{2}u_s(\vec{0}) \;=\; \sum_r \left[\sum_{z,x_{\rm op}} \frac{1}{2}\,\vec{x}_{\rm op}\times\bar{u}_{s'}(\vec{0})\,i\vec{\mathcal{F}}^C\Big(\vec{0};x=-\frac{r}{2},y=+\frac{r}{2},z,x_{\rm op}\Big)\,u_s(\vec{0})\right]$$

- The initial and final muon states are plane waves instead of properly normalized states.
- Recall the definition for $\mathcal{F}_\mu$, we sum all the internal points over the entire space time except we fix $x+y=0$.
- The time coordinate of the current, $(x_{\rm op})_0$ is integrated instead of being held fixed.

These features allow us to perform the lattice simulation efficiently in finite volume.

Note that we use the average of the two sampled points, $\frac{1}{2}(x+y)$, as the reference point (origin) for the moment method.

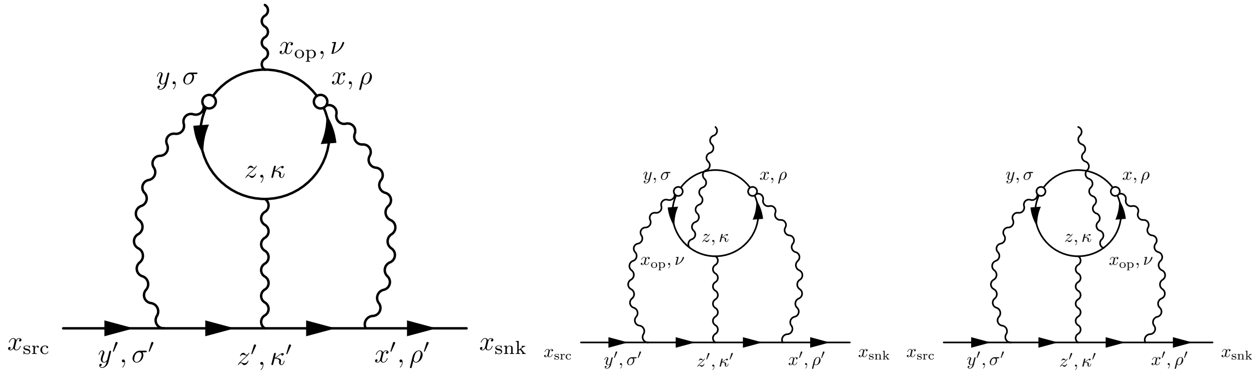

$$\frac{F_2(0)}{m}\,\bar{u}_{s'}(\vec{0})\frac{\vec{\Sigma}}{2}u_s(\vec{0})$$
$$= \sum_r \left[\sum_{z,x_{\rm op}} \frac{1}{2}\,\vec{x}_{\rm op}\times\bar{u}_{s'}(\vec{0})\,i\vec{\mathcal{F}}^C\Big(\vec{0};x=\frac{-r-z}{2},y=\frac{r-z}{2},z,x_{\rm op}\Big)\,u_s(\vec{0})\right] \qquad (17)$$

Instead of using the average of the two sampled points, $\frac{1}{2}(x+y)$, as the reference point (origin) for the moment method, we may also use the average of all three points $\frac{1}{3}(x+y+z)$ as the reference point (origin). The formula changes slightly and has the above form.

Then, all the three diagrams shown above become equivalent. We can then only evaluate only the first diagram with two point source propagators and no sequential propagators. **Phys.Rev. D93 (2016) no.1, 014503**

We plan to test this method with the infinite volume QED formulation.

Outline

- Introduction
- Lattice method
- HLbL on lattice
- **Disconnected diagrams**
- Finite volume effects
- π^0 contribution
- Summary and Future plans

Disconnected diagrams

- One diagram (the biggest diagram below) do not vanish even in the SU(3) limit.
- We extend the method and computed this leading disconnected diagram as well.

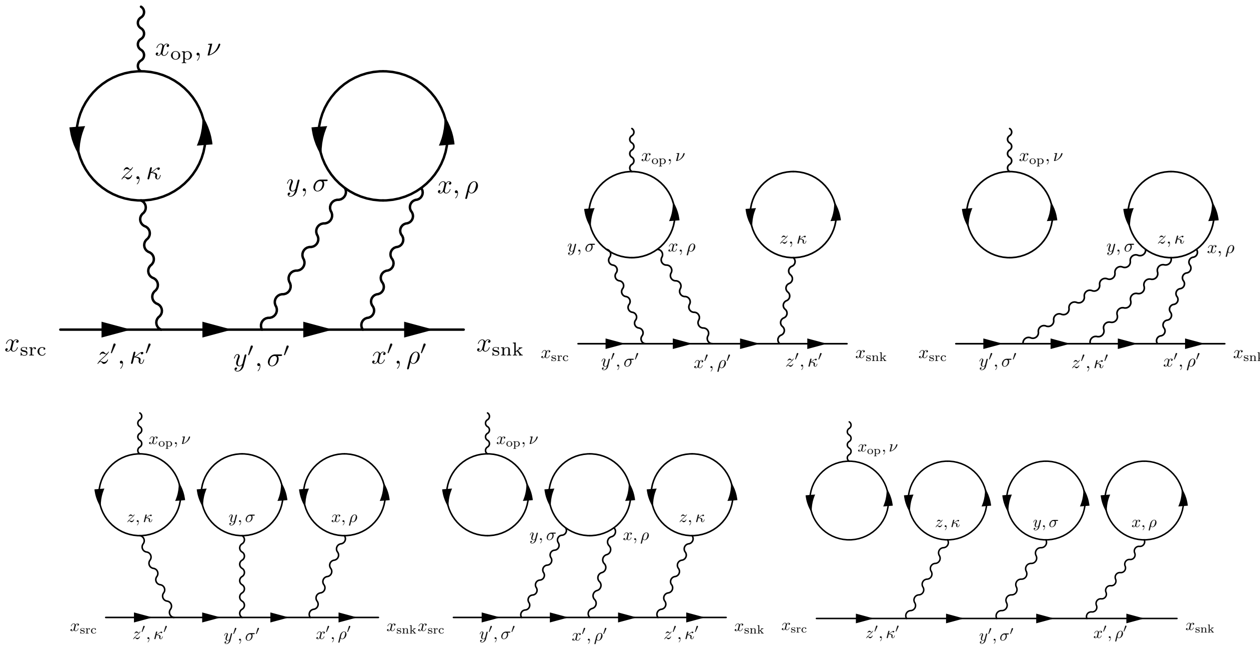

- Permutations of the three internal photons are not shown.
- There should be gluons exchange between and within the quark loops, but are not drawn.
- We need to make sure that the loops are connected by gluons by "vacuum" subtraction. So the diagrams are 1-particle irreducible.

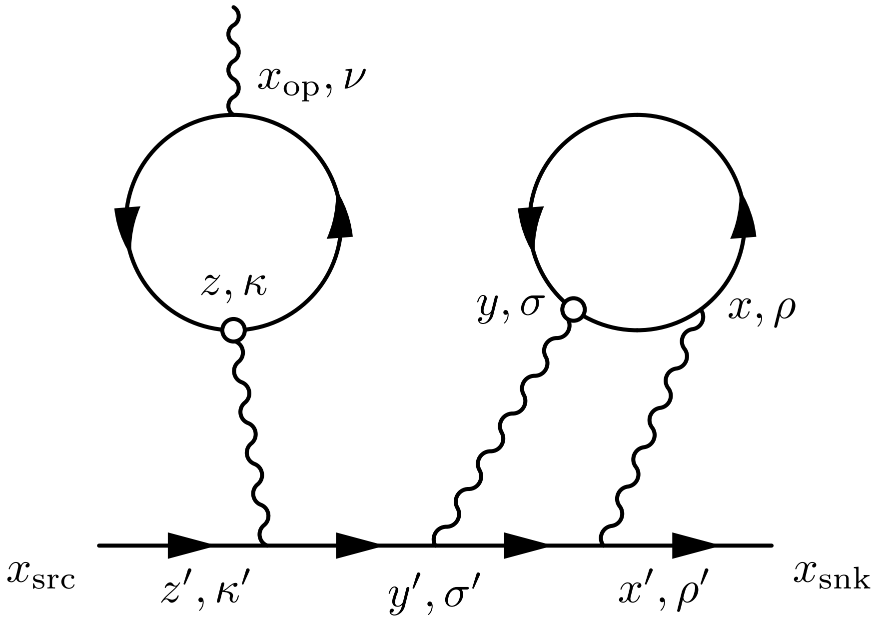

- Currently we have only calculated the leading disconnected diagram.
- Point z is used as the reference point (origin) for the moment method.
- We can use two point source photons at y and z, which are chosen randomly. The points $x_{\rm op}$ and x are summed over exactly on lattice.
- Only point source quark propagators are needed. We compute M point source propagators and all M^2 combinations of them are used to perform the stochastic sum over $r = z - y$.

Disconnected formula

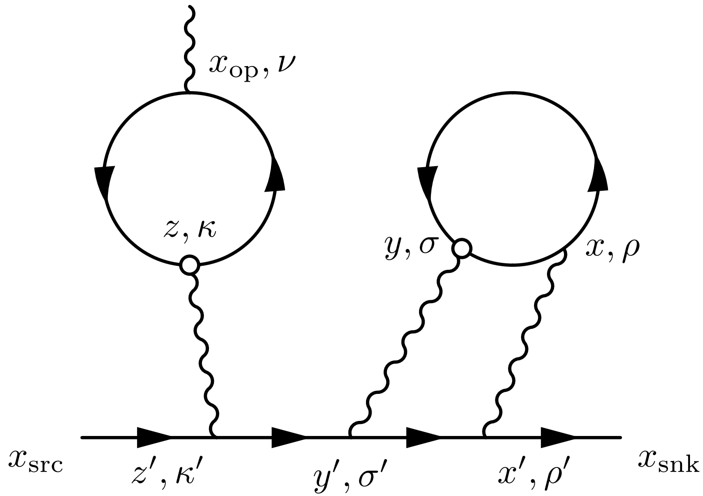

$$\frac{F_2^{\rm dHLbL}(0)}{m} \frac{(\sigma_{s',s})_i}{2} = \sum_{r,x} \sum_{x_{\rm op}} \frac{1}{2} \epsilon_{i,j,k} (x_{\rm op})_j \cdot i\, \bar{u}_{s'}(\vec{0})\, \mathcal{F}^D_k(x, y=r, z=0, x_{\rm op}) u_s(\vec{0}) \quad (18)$$

$$\mathcal{F}^D_\nu(x, y, z, x_{\rm op}) = (-i e)^6\, \mathcal{G}_{\rho,\sigma,\kappa}(x, y, z) \mathcal{H}^D_{\rho,\sigma,\kappa,\nu}(x, y, z, x_{\rm op}) \quad (19)$$

$$\mathcal{H}^D_{\rho,\sigma,\kappa,\nu}(x, y, z, x_{\rm op}) = \left\langle \frac{1}{2} \Pi_{\nu,\kappa}(x_{\rm op}, z) \left[\Pi_{\rho,\sigma}(x, y) - \Pi^{\rm avg}_{\rho,\sigma}(x-y)\right] \right\rangle_{\rm QCD} \quad (20)$$

$$\Pi_{\rho,\sigma}(x, y) = -\sum_q (e_q/e)^2\, {\rm Tr}[\gamma_\rho S_q(x, y)\, \gamma_\sigma S_q(y, x)]. \quad (21)$$

Outline

- Introduction
- Lattice method
- HLbL on lattice
- Disconnected diagrams
- **Finite volume effects**
- π^0 contribution
- Summary and Future plans

$$\mathcal{F}^C_\nu(x,y,z,x_{\rm op}) \;=\; (-ie)^6\,\mathcal{G}_{\rho,\sigma,\kappa}(x,y,z)\mathcal{H}_{\rho,\sigma,\kappa,\nu}(x,y,z,x_{\rm op})$$

The QED part, $\mathcal{G}_{\rho,\sigma,\kappa}(x,y,z)$ can be evaluated in infinite volume QED box.

The QCD part, $\mathcal{H}_{\rho,\sigma,\kappa,\nu}(x,y,z,x_{\rm op})$ can be evaluated in a finite volume QCD box.

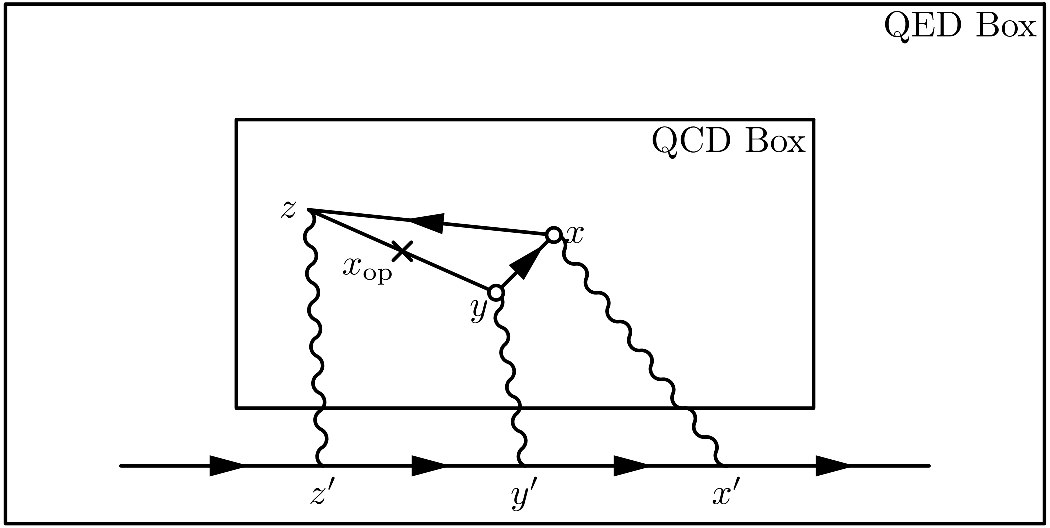

$$i^3\,\mathcal{G}_{\rho,\sigma,\kappa}(x,y,z) \;=\; \mathfrak{G}_{\rho,\sigma,\kappa}(x,y,z)+\mathfrak{G}_{\sigma,\kappa,\rho}(y,z,x)+\text{other 4 permutations.} \tag{22}$$

$$\mathfrak{G}_{\rho,\sigma,\kappa}(x,y,z) \;=\; e^{m_\mu(t_{\rm snk}-t_{\rm src})}\sum_{x',y',z'} G_{\rho,\rho'}(x,x')G_{\sigma,\sigma'}(y,y')G_{\kappa,\kappa'}(z,z') \tag{23}$$

$$\times\sum_{\vec{x}_{\rm snk},\vec{x}_{\rm src}} S_\mu(x_{\rm snk},x')i\gamma_{\rho'}S_\mu(x',y')i\gamma_{\sigma'}S_\mu(y',z')i\gamma_{\kappa'}S_\mu(z',x_{\rm src})$$

QCD finite volume effects

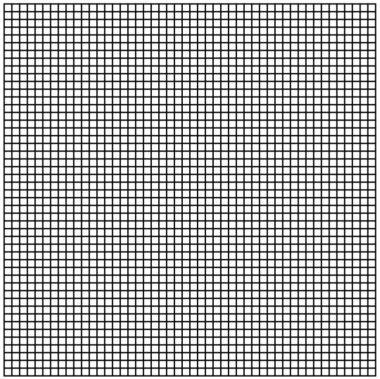

48I: $48^3 \times 96$, $5.5\,\mathrm{fm}$ box

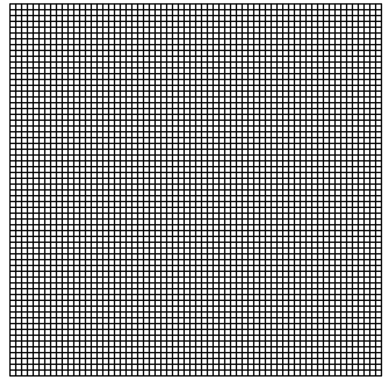

64I: $64^3 \times 128$, $5.5\,\mathrm{fm}$ box

Phys. Rev. D 93, 074505 (2016)

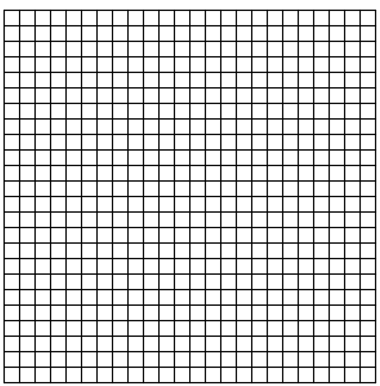

24D: $24^3 \times 64$, $4.8\,\mathrm{fm}$ box

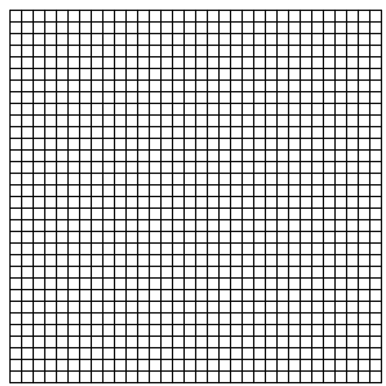

32D: $32^3 \times 64$, $6.4\,\mathrm{fm}$ box

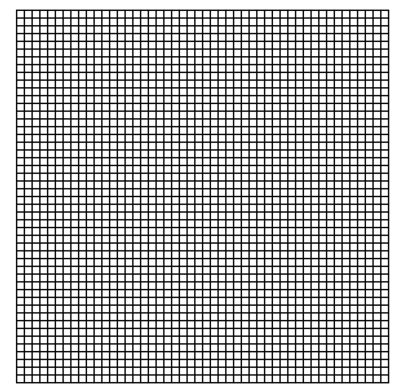

48D: $48^3 \times 64$, $9.6\,\mathrm{fm}$ box

32Dfine: $32^3 \times 64$, $4.8\,\mathrm{fm}$ box

Outline

- Introduction
- Lattice method
- HLbL on lattice
- Disconnected diagrams
- Finite volume effects
- **π^0 contribution**
- Summary and Future plans

We can separate the HLbL contribution into the short distance part:

$$\frac{F_2^{\text{short}}(0)}{m}\,\bar{u}_{s'}(\vec{0})\frac{\Sigma_i}{2}u_s(\vec{0})$$
$$= \frac{1}{V}\sum_{\substack{x,y,z \\ |x-y|,|y-z|,|x-z|\leqslant L_{\text{cut}}}}\sum_{x_{\text{op}}}\frac{1}{2}\epsilon_{i,j,k}(x_{\text{op}})_j\, i\mathcal{H}_{\rho,\sigma,\kappa,k}(x,y,z,x_{\text{op}})$$
$$\times\,\bar{u}_{s'}(\vec{0})(-ie)^6\,\mathcal{G}_{\rho,\sigma,\kappa}(x,y,z)\,u_s(\vec{0})$$

And the remaining long distance part, where at least two vector currents are separated by a distance longer than L_{cut}.

The short distance part can be evaluted on the lattice with relatively small finite volume error. For the long distance part, the hadronic 4 point function can be approximated by two major contribution: π^0 exchange and $\pi^\pm$ loop. We will start with the π^0 exchange diagram:

$$\mathcal{H}_{\rho,\sigma,\kappa,\nu}(x,y,z,x_{\text{op}}) \approx \sum_{u,v} F_{\rho,\sigma}(x,y,u)G_{\pi^0}(u,v)F_{\kappa,\nu}(z,x_{\text{op}},u) + \text{permuations} \tag{24}$$

Outline

- Introduction
- Lattice method
- HLbL on lattice
- Disconnected diagrams
- Finite volume effects
- π^0 contribution
- **Summary and future plans**

Summary and future plans

In a finite $(5.5\,\mathrm{fm})^3$ box with inverse lattice spacing $1/a = 1.73\,\mathrm{GeV}$, we obtained $a_\mu^{\mathrm{HLbL}} \times 10^{10} = 5.35 \pm 1.35$, except for some subleading disconnected diagrams.

- **Continuum limit**: Finish up the finite volume QED 64I calculation to extrapolate away the discretization error for the 48I results.
- **Connected infinite QED volume**: QCD part can reuse the previously saved data. Preliminary results are available now.
- **Leading disconnected infinite QED volume**: Still, we plan to reuse the previously saved data for the QCD part. We are exploring the method to suppress the statistics noise.
- **Sub-leading disconnected diagrams**: These diagrams vanishes in the flavor $\mathrm{SU}(3)$ limit. We plan to calculate these diagrams in the future.
- **Large physical QCD volume**: Study the QCD finite volume effects with the 24ID, 32ID, and 48ID ensemble. The 48I,64I and the 32IDfine ensembles can also help understand the discretization effects with these coarse ensembles.
- **Neutral pion contribution**: Study the contribution from the π^0 exchange at long distance. This could help estimate or reduce the QCD finite volume error of the direct lattice calculation.
- Final goal is reaching 10% accuracy to compare with the new experiments.

Thank You!

A New Hope

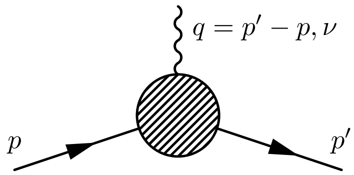

	$a_\mu \times 10^{10}$	Reference
Experiment	11659208.9 ± 6.3	E821, $g-2$ Collab. 2006
Standard Model	11659180.2 ± 3.9	Particle Data Group, 2014
???	28.7 ± 7.4	

Future is hard to predict, let's think of something similar in the history.

Precession of the perihelion of Mercury (in unit of arcsec/Julian century)

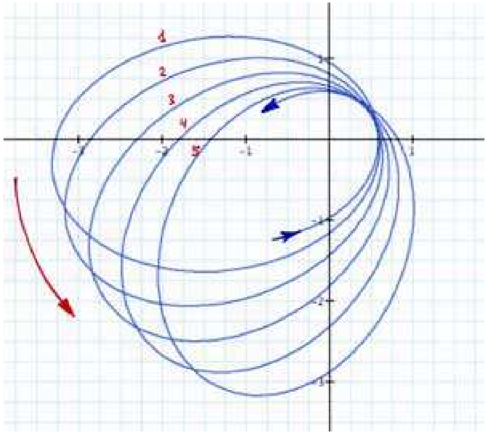

	Precession	Reference
Experiment	574.10 ± 0.65	G. M. Clemence 1947
Newton's Law	531.63 ± 0.69	G. M. Clemence 1947
???	42.47 ± 0.95	